GEOLOGY | THE GEOLOGICAL SOCIETY OF AMERICA®

https://doi.org/10.1130/G50046.1

Manuscript received 17 January 2022
Revised manuscript received 4 April 2022
Manuscript accepted 6 April 2022

Published online 12 May 2022

Seismic evidence for lithospheric boudinage and its implications for continental rifting

Luan C. Nguyen[1], Alan Levander[1], Fenglin Niu[1], Julia Morgan[1] and Guoliang Li[2]
[1]Department of Earth, Environmental and Planetary Sciences, Rice University, 6100 Main Street, Houston, Texas 77005, USA
[2]Computational Mathematics Science and Engineering, Michigan State University, 428 South Shaw Lane, East Lansing, Michigan 48824, USA

ABSTRACT

The continental rifting that precedes the breakup of a continent and the formation of a new ocean basin is one of the key processes of plate tectonics. Although often viewed as a two-dimensional process, rifted margins exhibit significant variations along strike. We document along-strike variations developed during the ca. 200–160 Ma continental rifting that formed the margins of the Gulf of Mexico ocean basin. Rayleigh-wave ambient noise tomography reveals a zone of high and low seismic velocity resembling large scale geologic boudins in the mantle lithosphere of the northwestern Gulf of Mexico margin. These features become progressively less prominent eastward following the transition from a magma-poor to a magma-rich passive margin. We infer that mantle refertilization and thickness of the pre-rift lithosphere control deformation style and the along-strike variations in continental rifting. Our results also suggest that deformation during rifting produces long-lived features that persist long after breakup and, therefore, can be used to study rifted margins globally.

INTRODUCTION

Rifted continental margins are often characterized as magma-rich or magma-poor depending on the degree of crustal volcanism and magmatism identified by geophysical analysis and seismic imaging (Whitmarsh et al., 2001; Menzies et al., 2002). What remains an enigma is the determining factor that controls melt intrusion and eruption at a particular margin; e.g., alternating volcanic and non-volcanic segments have been identified along the Atlantic Ocean margins. This pattern of variation in syn-rift volcanism has also been reported along the United States continental margin surrounding the Gulf of Mexico. To gain better understanding of the evolution of continental rifting and ocean basin formation, we imaged the lithospheric structure of the Gulf of Mexico and its continental margins using ambient noise Rayleigh surface waves.

The passive margins enclosing the Gulf of Mexico formed as a result of continental extension that began the separation of the North and South American plates beginning ~200 m.y. ago. The ensuing breakup at ca. 160 Ma formed the oceanic lithosphere of the Gulf of Mexico (Pindell, 1985; Sawyer et al., 1991). In this process, the offshore Gulf Coast in the northern Gulf of Mexico and the offshore Yucatan in the south formed as conjugate margins (Fig. 1). We developed a three-dimensional (3-D) shear wave velocity model that displays boudinage of the lithosphere under the continental margin of the northwestern Gulf of Mexico. Geologic boudinage refers to the pinch-and-swell structures (boudins) associated with the extension of a viscously stratified rock body (Ricard and Froidevaux, 1986). The presence of these structures provides insight to the mechanical properties of the lithosphere in an extensional setting. Our analysis in combination with previous findings demonstrate geologic boudins play an important role in enhancing localized deformation and asymmetric geometry of rifted margins. We infer that boudinage development is influenced by inherited thickness of the lithosphere and by the process of mantle refertilization triggered by melt infiltration from the ascending asthenosphere during rifting.

METHOD

The data analyzed in this study were recorded by 566 seismic stations in the continental United States and Mexico, and several stations located in and around Cuba. We cross-correlated the vertical component of the noise field for periods of 15–95 s (frequencies of 0.011–0.067 Hz). This combined data set (Fig. S1a in the Supplemental Material[1]) ensures sufficient areal coverage of the study area and allows for estimation of Vs to a depth of 150 km, imaging much of the lithosphere-asthenosphere system. Our general processing workflow was adopted from Bensen et al. (2007). Daily cross-correlations were performed between station pairs having contemporaneous records. For each station pair, all daily cross-correlations were linearly stacked to produce a final cross-correlation function. The empirical Green's function was extracted from this function using the frequency-time analysis method (Levshin and Ritzwoller, 2001). Only correlations with a signal-to-noise ratio greater than 10 were accepted, keeping the uncertainty in phase-velocity measurement to 35–50 m/s or ~1% (Bensen et al., 2007). Using these measurements of average phase-velocities, we performed 2-D phase-velocity tomography on a half-degree grid with a total of 1591 nodes (Fig. S1b). At each grid node, the calculated phase-velocity was inverted for a 1-D shear-wave velocity profile using a Monte Carlo Markov Chain inversion scheme (Afonso et al., 2013). The final 3-D shear-wave velocity model was computed by interpolating the 1-D models over the entire grid.

RESULTS

Sensitivity kernel analysis shows that the long-period phase velocity data can resolve

[1]Supplemental Material. Discussion of the origin of the reduced velocity in the mantle lithosphere, data coverage, and sensitivity tests. Please visit https://doi.org/10.1130/GEOL.S.19633149 to access the supplemental material, and contact editing@geosociety.org with any questions.

CITATION: Nguyen, L.C., et al., 2022, Seismic evidence for lithospheric boudinage and its implications for continental rifting: Geology, v. XX, p. , https://doi.org/10.1130/G50046.1

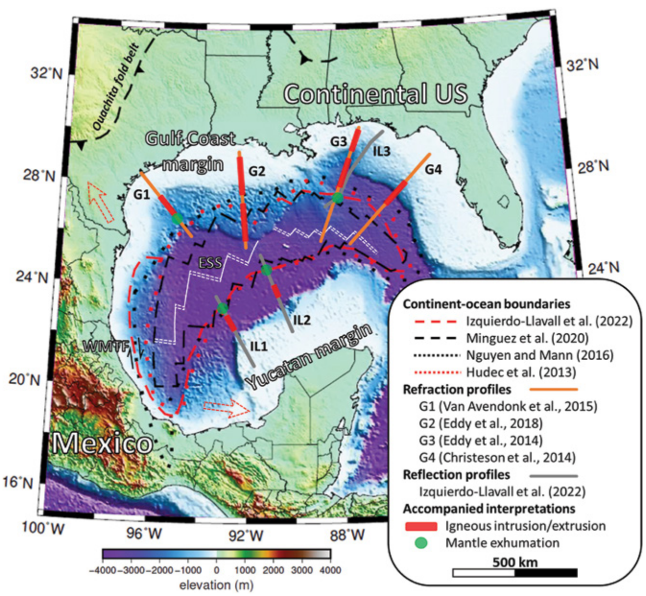

Figure 1. Geographic setting of the Gulf of Mexico, including the central ocean basin and the surrounding continental margins. Select seismic refraction and reflection profiles from previous studies are shown (orange and gray lines, respectively) along with their interpreted zones of mantle exhumation and magmatic intrusion/extrusion. Red arrows mark our inferred orientation of the Mesozoic continental rifting. ESS—extinct spreading system; WMTF—Western Main Transform Fault (Nguyen and Mann, 2016).

structures to ~200 km depth, while checkerboard tests indicate that our data set has a lateral resolution of ~50 km (the grid spacing of the 2-D tomography) (Fig. S1). We identified the Moho at depths comparable to refraction results from previous studies (Fig. S2). At greater depths, the continental lithospheric mantle generally exhibits a higher shear-wave velocity (Vs) (4.2–4.69 km/s, average of 4.58 km/s) than the oceanic lithospheric mantle beneath the Gulf of Mexico (4.2–4.65 km/s, average of 4.54 km/s) (Fig. 2). This is consistent with global Vs observations that show continental lithosphere systematically faster than its oceanic counterpart (Fischer et al., 2010). The drop in Vs over the oceanic region can be attributed to the variation in degree of mantle depletion, which can produce more than 2% difference in Vs (Lee, 2003).

The pervasive low upper-mantle Vs onshore in northeastern Mexico where Vs in the continental mantle drops below 4.5 km/s (Fig. 2B) is attributed to shallow asthenosphere in the slab window formed by subduction of the Farallon plate beneath North America (van der Lee and Nolet, 1997). In contrast, beneath the offshore northwestern Gulf of Mexico passive margin, we identify linear anomalies of reduced Vs in the mantle lithosphere (Fig. 2) with a northeast-southwest strike (dotted lines in Fig. 2) The velocity reduction is greatest in the west (−2%) and diminishes to the east. In dip cross sections, the velocity anomalies exhibit the characteristic swell-and-necking geometry (Fig. 3A) of geologic boudinage seen in surface outcrop (Ramberg, 1955) and tomographically imaged as subducting slab segmentation (Gerya et al., 2021). The lithospheric boudins have a thickness and wavelength of ~40 km and ~120 km, respectively, and are centered at a depth of 75 km. The area with lowest Vs (~4.50 km/s) is found in the necking zones, whereas Vs in the thickest section of the boudin is slightly higher (~4.54 km/s). Compared to the maximum Vs (~4.69 km/s) observed in the U.S. continental mantle lithosphere and the offshore Yucatan margin along the three profiles in Figure 3, the velocity in the boudins' swell and pinch zones are reduced by 3.0% and 4.0%, respectively. We examined the effect of parameterization on the

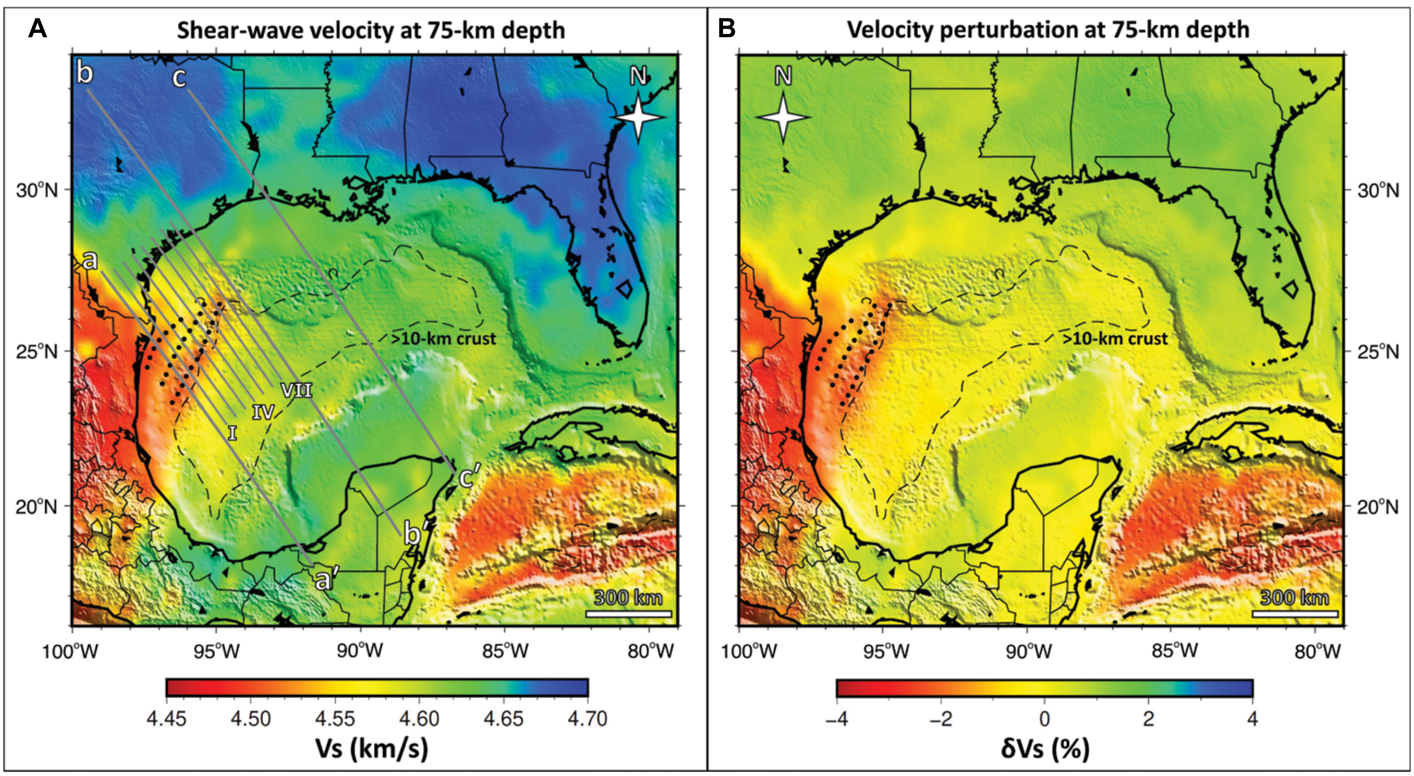

Figure 2. Depth slice (at 75 km) through our inverted 3-D model showing shear-wave velocity (A) and velocity perturbation computed from the inverted mean velocity at this depth (B). Black dotted lines trace the pinches and swells of the mantle lithosphere. The necking zones exhibits lowest Vs values. Gray lines in A mark the location of cross sections shown in Figure 3. Dashed outline marks the 10-km-thickness contour of igneous crust derived from our Vs model. Crustal thickness inside the contour is ~7.8 km on average.

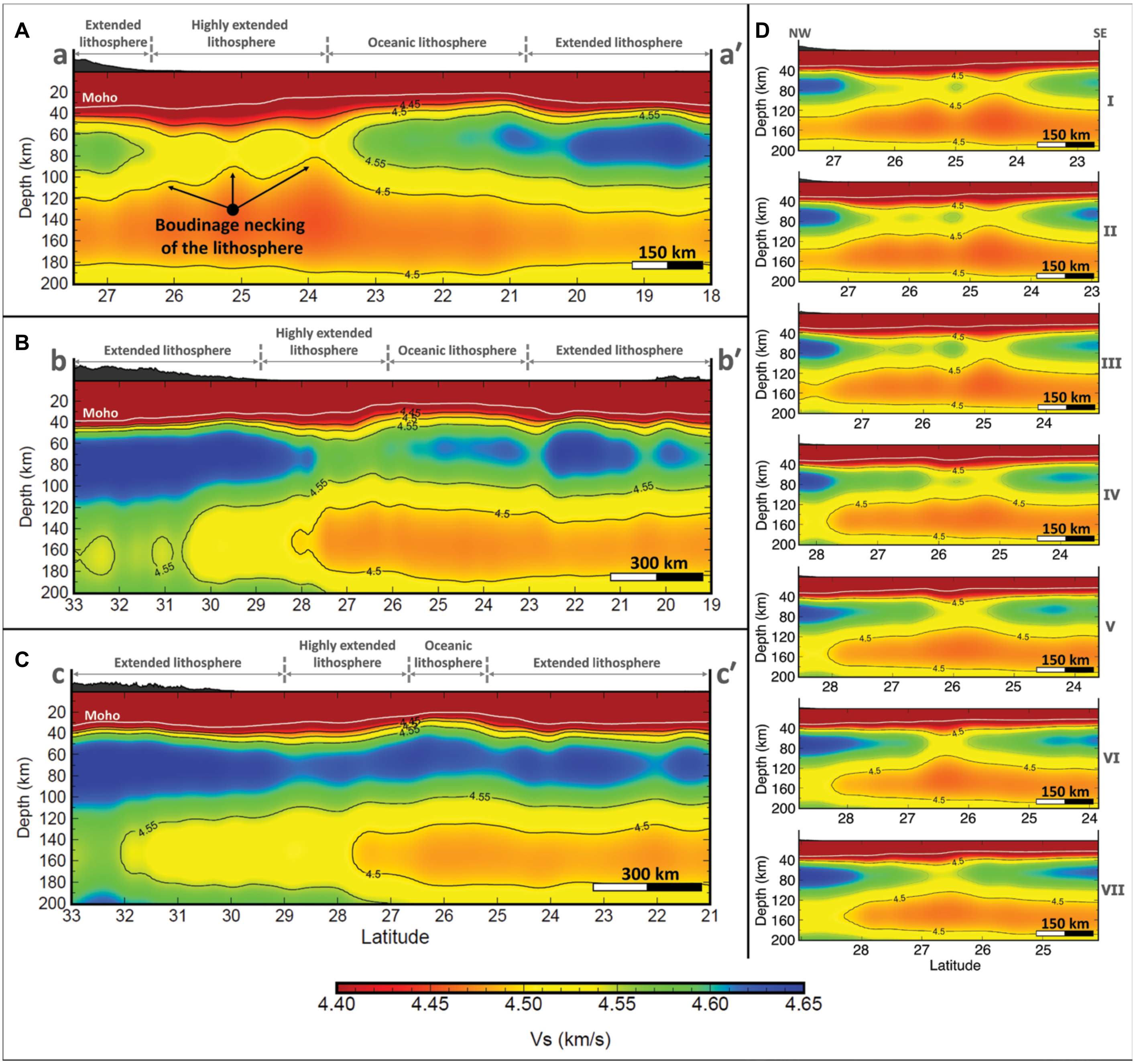

Figure 3. Shear-wave velocity across ten northwest-southeast profiles shown in Figure 2A. Velocity at shallow depth is saturated at 4.4 km/s. The Moho is taken at the 4.2 km/s contour of the Vs model. Interpretation of various geologic domains is based on crustal thickness and Vs in the mantle lithosphere. Eastward gradation of the lithospheric boudinage is shown in D.

inversion and determined that these anomalies are robust features. The velocity reduction at the boudin's swell and pinch persists under different parameterizations of the inversion. The swell-and -pinch structures are reflected in the measured dispersion curves at various grid points (Fig. S3), which consistently show lower phase velocities at the pinch zones compared to the swells, especially at wave periods above 50 s. Our tests confirm that this reduction in phase velocities reflects structural variation in the mantle lithosphere and not in the crust (Fig. S4; Tables S1 and S2). Similar to the trend seen in Figure 2, profiles I–VII (Fig. 3D) demonstrate that both the magnitude of Vs anomaly and boudinage geometry become less prominent eastward along the Gulf Coast margin (GCM). Nevertheless, the boudinage can be traced as a persistent feature ~400 km along the margin (Fig. 2).

Part of the boudinage feature lies within a region of uncertainty where previous interpretations of the continent-ocean boundary do not agree well (Fig. 1), partially due to the lack of deep seismic constraints there. Depending on the continent-ocean boundary location, our mapped boudinage occupies either oceanic lithosphere (Nguyen and Mann, 2016; Izquierdo-Llavall et al., 2022) or continental lithosphere (Hudec et al., 2013; Minguez et al., 2020). Nevertheless, based on the crustal thickness derived from our Vs model, this feature lies well within the area where the igneous crust is >10 km thick, while most of the oceanic Gulf of Mexico has an average crustal thickness of ~7.8 km (Fig. 2). Therefore, we conclude that the boudinage is most likely of continental origin and formed within the highly extended continental domain. As discussed below, we interpret the east-west variation in the boudinage structure as a reflection of differential extension controlled by inherited thickness of the lithosphere prior to rifting.

DISCUSSION

Origin of the Reduced Velocity in the Mantle Lithosphere

We consider several mechanisms that can reduce shear-wave velocity within the mantle lithosphere (see the Supplemental Material). We interpret the observed velocity reduction as evidence of extensional deformation, possibly with syn-rift magmatic intrusion in the lower lithosphere. Extensional deformation can lead to formation of geologic boudinage and to reduction in shear-wave velocity. Stretching of a rheologically layered body results in instability of the strong, competent layer that deforms into the discrete lozenges making up the boudins. Often seen at shallow crustal levels (Clerc et al., 2018; Deng et al., 2020), lithospheric-scale boudinage has been suggested in the central Mediterranean back arc (Gueguen et al., 1997), and identified along the down-going plate in subduction zones (Lister et al., 2008; Gerya et al., 2021). The boudins form by localization of deformation, i.e., shearing and faulting, at their peripheries. Mantle rock under extensional stress also becomes weaker at depths and temperatures where dislocation creep gives way to diffusion creep as the dominant deformation mechanism (Karato and Wu, 1993), which causes grain-size reduction and reduced shear modulus (Faul and Jackson, 2005).

We attribute the largest reduction in Vs observed at the pinch areas of the boudins to grain-size reduction and the development of localized shear zones during rifting. Once initiated, shear zones lead to further grain-size reduction and promote weakening of the mantle lithosphere in a feedback. Hence, the necking regions of the boudins become areas with the most deformation and lowest shear-wave velocity. At 1300 °C, a grain-size reduction from 10 mm to 1 mm, the maximum threshold where diffusion creep can be established (Hopper and Buck, 1993), results in an ~10% decrease in shear modulus corresponding to a Vs reduction of ~5%. This is the same magnitude as the observed 1%–3% reduced Vs in the boudin necks. Above the boudinage, there is an observable correlation of variation in Moho depth and the boudin necks. Locations where the Moho dips seaward are laterally offset from the pinch zones in the mantle such that they could be linked by oblique shear zones extending from the Moho down through the boudin necks (Fig. S6).

A process that could enhance the development of shear zones is the local weakening of the lithosphere by mantle refertilization: basaltic melts infiltrate and enrich depleted harzburgite to lherzolite (Foley, 2008; Casagli et al., 2017). The enriched lithosphere is weaker with a lower shear velocity. Evidence for rejuvenation of the mantle lithosphere during Mesozoic rifting has been found in Gulf of Mexico mantle xenoliths collected along the coast of Louisiana (Stern et al., 2011), at approximately the longitude that the margin transitions from magma-poor to magma-rich. We propose that during the Triassic-Jurassic rifting event, the lithosphere was first deformed under pure shear and experienced initial grain-size reduction. The lithosphere thinned locally and was intruded by basaltic melts made possible by asthenosphere ascent under the thinning lithosphere. Zones of melt intrusion then became loci for additional deformation, ultimately the boudin necks, as continental rifting evolved into the simple shear process that created the asymmetric conjugate margins (Fig. 4).

Implications for Lithospheric Extension and Upper Mantle Rheology

The observed gradual fading of the boudinage toward the northeastern Gulf of Mexico appears to correspond with an eastward trend of increasing syn-rift magmatism. The western side of the margin has been characterized as nonvolcanic, with exhumed mantle (Van Avendonk et al., 2015) whereas syn-rift magmatism and volcanism are increasingly prominent toward the east (Christeson et al., 2014; Eddy et al., 2014, 2018). Furthermore, the crustal stretching factor demonstrates that the rift zone is narrower at longitude W90° and broadens eastward at longitude W96° (Fig. S7).

Stretching of a thick and strong lithosphere can result in a narrower rift (Kogan et al., 2012), lithospheric necking, and possibly mantle exhumation (Brun and Beslier, 1996). To explain why crustal volcanism and magmatism are more widespread in the eastern GCM, we suggest that the pre-rift lithosphere was thicker in the western GCM than under the Ouachita orogeny indenter that occupies the central and eastern GCM. In addition to melt generation being suppressed by a thicker lithosphere (Zheng et al., 2015), surface eruption of a small volume of melts generated during extension is hindered by the great thickness of the overlying lithosphere, allowing mantle refertilization at depth, weakening of the lithosphere, and increased deformation. As boudins with the reduced Vs result from extension and melt-induced deformation, their near absence in the conjugate Yucatan margin suggests asymmetric rifting was facilitated by focused shear zone(s). Such an asymmetry is also clearly observed at the crustal level between the two conjugate margins (Fig. S7).

While most numerical simulations of rifting attribute localized shear zones to preexisting heterogeneity in the lithosphere, our result suggests that this assumption is not necessary if the mantle is locally refertilized. Enriching and weakening the mantle lithosphere at discrete regions would trigger localized deformation that forms boudin necks. One of the necking regions can become the dominant shear zone that facilitates rifting in an asymmetric fashion (Fig. 4). Mineral grain growth occurring post-deformation or during diffusion creep can act as a "healing" agent that strengthens a former damaged zone. However, the fact that reduced Vs is observed in the boudinage necks suggests that grain growth might not be as effective as previously predicted, consistent with recent findings (Speciale et al., 2020), and in agreement with the observations of shear zones preserved in exhumed upper mantle with grain sizes of <1 mm (Warren and Hirth, 2006). This is an important observation, because these long-lived features can be used to interpret geologic structures and processes at other rifted margins globally.

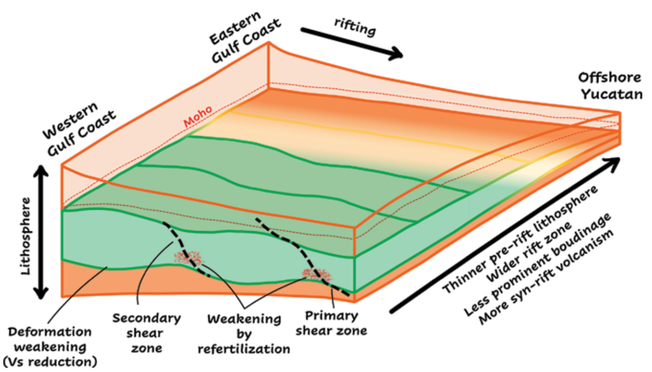

Figure 4. Schematic illustration depicting lithospheric thickness and strength as a controlling factor in the development of large-scale boudinage in the mantle lithosphere. Regions of reduced Vs are shown in green and inferred to be results of the transition in creep mechanism during extensional deformation. Necking of the lithospheric mantle is induced by development of localized shear zones in an area of mantle refertilization from intruding asthenospheric melt trapped within a thick lithosphere (red spots). A primary shear zone can grow to accommodate asymmetric breakup between the conjugate margins. Toward the eastern Gulf Coast, original lithospheric thickness is inferred to be lower than in the west, such that extension is more widely distributed and melt generation and eruption are more prominent. Without weakening from mantle refertilization, deep shear zones are less likely to initiate; thus, the gradual fading of boudinage and Vs reduction eastward.

ACKNOWLEDGMENTS

We thank Wenpei Miao for his assistance in the initial data organizing and processing. We thank Xyoli Pérez Campos for her help in accessing the seismic records from the Mexico National Seismological

Service. Seismic data were downloaded through the IRIS Wilber 3 system (https://ds.iris.edu/wilber3/) or IRIS Web Services (https://service.iris.edu/). The list of seismic networks can be found in the Supplemental Material. SSN data were obtained by the Servicio Sismológico Nacional (México), station maintenance, data acquisition and distribution are thanks to its personnel. We are thankful for the constructive comments from Harm Van Avendonk, François Sapin, and an anonymous reviewer in their reviews of this work.

REFERENCES CITED

Afonso, J.C., Fullea, J., Griffin, W.L., Yang, Y., Jones, A.G., Connolly, J.A.D., and Reilly, S.Y.O., 2013, 3-D multi-observable probabilistic inversion for the compositional and thermal structure of the lithosphere and upper mantle. I: A priori petrological information and geophysical observables: Journal of Geophysical Research: Solid Earth, v. 118, p. 2586–2617, https://doi.org/10.1002/jgrb.50124.

Bensen, G.D., Ritzwoller, M.H., Barmin, M.P., Levshin, A.L., Lin, F., Moschetti, M.P., Shapiro, N.M., and Yang, Y., 2007, Processing seismic ambient noise data to obtain reliable broad-band surface wave dispersion measurements: Geophysical Journal International, v. 169, p. 1239–1260, https://doi.org/10.1111/j.1365-246X.2007.03374.x.

Brun, J.P., and Beslier, M.O., 1996, Mantle exhumation at passive margins: Earth and Planetary Science Letters, v. 142, p. 161–173, https://doi.org/10.1016/0012-821X(96)00080-5.

Casagli, A., Frezzotti, M.L., Peccerillo, A., Tiepolo, M., and De Astis, G., 2017, (Garnet)-spinel peridotite xenoliths from Mega (Ethiopia): Evidence for rejuvenation and dynamic thinning of the lithosphere beneath the southern Main Ethiopian Rift: Chemical Geology, v. 455, p. 231–248, https://doi.org/10.1016/j.chemgeo.2016.11.001.

Christeson, G.L., Van Avendonk, H.J.A., Norton, I.O., Snedden, J.W., Eddy, D.R., Karner, G.D., and Johnson, C.A., 2014, Deep crustal structure in the eastern Gulf of Mexico: Journal of Geophysical Research: Solid Earth, v. 119, p. 6782–6801, https://doi.org/10.1002/2014JB011045.

Clerc, C., Ringenbach, J.C., Jolivet, L., and Ballard, J.F., 2018, Rifted margins: Ductile deformation, boudinage, continentward-dipping normal faults and the role of the weak lower crust: Gondwana Research, v. 53, p. 20–40, https://doi.org/10.1016/j.gr.2017.04.030.

Deng, H., Ren, J., Pang, X., Rey, P.F., McClay, K.R., Watkinson, I.M., Zheng, J., and Luo, P., 2020, South China Sea documents the transition from wide continental rift to continental break up: Nature Communications, v. 11, p. 4583, https://doi.org/10.1038/s41467-020-18448-y.

Eddy, D.R., Van Avendonk, H.J.A., Christeson, G.L., Norton, I.O., Karner, G.D., Johnson, C., and Snedden, J.W., 2014, Deep crustal structure of the northeastern Gulf of Mexico: Implications for rift evolution and seafloor spreading: Journal of Geophysical Research: Solid Earth, v. 119, p. 6802–6822, https://doi.org/10.1002/2014JB011311.

Eddy, D.R., Van Avendonk, H.J.A., Christeson, G.L., and Norton, I.O., 2018, Structure and origin of the rifted margin of the northern Gulf of Mexico: Geosphere, v. 14, p. 1804–1817, https://doi.org/10.1130/GES01662.1.

Faul, U.G., and Jackson, I., 2005, The seismological signature of temperature and grain size variations in the upper mantle: Earth and Planetary Science Letters, v. 234, p. 119–134, https://doi.org/10.1016/j.epsl.2005.02.008.

Fischer, K.M., Ford, H.A., Abt, D.L., and Rychert, C.A., 2010, The lithosphere-asthenosphere boundary: Annual Review of Earth and Planetary Sciences, v. 38, p. 551–575, https://doi.org/10.1146/annurev-earth-040809-152438.

Foley, S.F., 2008, Rejuvenation and erosion of the cratonic lithosphere: Nature Geoscience, v. 1, p. 503–510, https://doi.org/10.1038/ngeo261.

Gerya, T.V., Bercovici, D., and Becker, T.W., 2021, Dynamic slab segmentation due to brittle-ductile damage interactions in the outer rise: Nature, v. 599, p. 245–250, https://doi.org/10.1038/s41586-021-03937-x.

Gueguen, E., Doglioni, C., and Fernandez, M., 1997, Lithospheric boudinage in the western Mediterranean back-arc basin: Terra Nova, v. 9, p. 184–187, https://doi.org/10.1046/j.1365-3121.1997.d01-28.x.

Hopper, J.R., and Buck, W.R., 1993, The initiation of rifting at constant tectonic force: Role of diffusion creep: Journal of Geophysical Research, v. 98, p. 16213–16221, https://doi.org/10.1029/93JB01725.

Hudec, M.R., Norton, I.O., Jackson, M.P.A., and Peel, F.J., 2013, Jurassic evolution of the Gulf of Mexico salt basin: American Association of Petroleum Geologists Bulletin, v. 97, p. 1683–1710, https://doi.org/10.1306/04011312073.

Izquierdo-Llavall, E., Ringenbach, J.C., Sapin, F., Rives, T., and Callot, J.P., 2022, Crustal structure and lateral variations in the Gulf of Mexico conjugate margins: From rifting to break-up: Marine and Petroleum Geology, v. 136, p. 105484, https://doi.org/10.1016/j.marpetgeo.2021.105484.

Karato, S.I., and Wu, P., 1993, Rheology of the upper mantle: A synthesis: Science, v. 260, p. 771–778, https://doi.org/10.1126/science.260.5109.771.

Kogan, L., Fisseha, S., Bendick, R., Reilinger, R., McClusky, S., King, R., and Solomon, T., 2012, Lithospheric strength and strain localization in continental extension from observations of the East African Rift: Journal of Geophysical Research: Solid Earth, v. 117, B03402, https://doi.org/10.1029/2011JB008516.

van der Lee, S., and Nolet, G., 1997, Upper mantle S velocity structure of North America: Journal of Geophysical Research: Solid Earth, v. 102, p. 22,815–22,838, https://doi.org/10.1029/97JB01168.

Lee, C.-T.A., 2003, Compositional variation of density and seismic velocities in natural peridotites at STP conditions: Implications for seismic imaging of compositional heterogeneities in the upper mantle: Journal of Geophysical Research: Solid Earth, v. 108, p. 2441, https://doi.org/10.1029/2003jb002413.

Levshin, A.L., and Ritzwoller, M.H., 2001, Automated detection, extraction, and measurement of regional surface waves: Pure and Applied Geophysics, v. 158, p. 1531–1545, https://doi.org/10.1007/PL00001233.

Lister, G., Kennett, B., Richards, S., and Forster, M., 2008, Boudinage of a stretching slablet implicated in earthquakes beneath the Hindu Kush: Nature Geoscience, v. 1, p. 196–201, https://doi.org/10.1038/ngeo132.

Menzies, M.A., Klemperer, S.L., Ebinger, C.J., and Baker, J., 2002, Characteristics of volcanic rifted margins, *in* Menzies, M.A., et al., eds., Volcanic Rifted Margins: Geological Society of America Special Paper 362, p. 1–14, https://doi.org/10.1130/0-8137-2362-0.1.

Minguez, D., Gerald Hensel, E., and Johnson, E.A.E., 2020, A fresh look at Gulf of Mexico tectonics: Testing rotations and breakup mechanisms from the perspective of seismically constrained potential-fields modeling and plate kinematics: Interpretation (Tulsa), v. 8, p. SS31–SS45, https://doi.org/10.1190/INT-2019-0256.1.

Nguyen, L.C., and Mann, P., 2016, Gravity and magnetic constraints on the Jurassic opening of the oceanic Gulf of Mexico and the location and tectonic history of the Western Main transform fault along the eastern continental margin of Mexico: Interpretation (Tulsa), v. 4, p. SC23–SC33, https://doi.org/10.1190/INT-2015-0110.1.

Pindell, J.L., 1985, Alleghenian reconstruction and subsequent evolution of the Gulf of Mexico, Bahamas, and Proto-Caribbean: Tectonics, v. 4, p. 1–39, https://doi.org/10.1029/TC004i001p00001.

Ramberg, H., 1955, Natural and experimental boudinage and pinch-and-swell structures: The Journal of Geology, v. 63, p. 512–526, https://doi.org/10.1086/626293.

Ricard, Y., and Froidevaux, C., 1986, Stretching instabilities and lithospheric boudinage: Journal of Geophysical Research, v. 91, p. 8314–8324, https://doi.org/10.1029/JB091iB08p08314.

Sawyer, D.S., Buffler, R.T., and Pilger, R.H.J., 1991, The crust under the Gulf of Mexico basin, *in* Salvador, A. ed., The Gulf of Mexico Basin: Boulder, Colorado, Geological Society of America, The Geology of North America, v. J, p. 53–72, https://doi.org/10.1130/DNAG-GNA-J.53.

Speciale, P.A., Behr, W.M., Hirth, G., and Tokle, L., 2020, Rates of olivine grain growth during dynamic recrystallization and postdeformation annealing: Journal of Geophysical Research: Solid Earth, v. 125, e2020JB020415, https://doi.org/10.1029/2020JB020415.

Stern, R.J., Anthony, E.Y., Ren, M., Lock, B.E., Norton, I., Kimura, J.I., Miyazaki, T., Hanyu, T., Chang, Q., and Hirahara, Y., 2011, Southern Louisiana salt dome xenoliths: First glimpse of Jurassic (ca. 160 Ma) Gulf of Mexico crust: Geology, v. 39, p. 315–318, https://doi.org/10.1130/G31635.1.

Van Avendonk, H.J.A., Christeson, G.L., Norton, I.O., and Eddy, D.R., 2015, Continental rifting and sediment infill in the northwestern Gulf of Mexico: Geology, v. 43, p. 631–634, https://doi.org/10.1130/G36798.1.

Warren, J.M., and Hirth, G., 2006, Grain size sensitive deformation mechanisms in naturally deformed peridotites: Earth and Planetary Science Letters, v. 248, p. 438–450, https://doi.org/10.1016/j.epsl.2006.06.006.

Whitmarsh, R.B., Manatschal, G., and Minshull, T.A., 2001, Evolution of magma-poor continental margins from rifting to seafloor spreading: Nature, v. 413, p. 150–154, https://doi.org/10.1038/35093085.

Zheng, J.P., Lee, C.T.A., Lu, J.G., Zhao, J.H., Wu, Y.B., Xia, B., Li, X.Y., Zhang, J.F., and Liu, Y.S., 2015, Refertilization-driven destabilization of subcontinental mantle and the importance of initial lithospheric thickness for the fate of continents: Earth and Planetary Science Letters, v. 409, p. 225–231, https://doi.org/10.1016/j.epsl.2014.10.042.

Printed in USA